Available online at www.sciencedirect.com
SCIENCE DIRECT®
Tetrahedron: Asymmetry
Tetrahedron: *Asymmetry* 15 (2004) 1431–1436

α,α′-Bis(trifluoromethyl)-9,10-anthracenedimethanol: enantioselective synthesis and bidentate complexes with benzenedimethanols

Carla Estivill, Petko M. Ivanov, Marta Pomares, Marta Sánchez-Arís and Albert Virgili*

Departament de Química, Universitat Autònoma de Barcelona, 08193 Bellaterra, Barcelona, Spain

Received 20 January 2004; revised 10 March 2004; accepted 12 March 2004

Available online 9 April 2004

Abstract—α,α′-Bis(trifluoromethyl)-9,10-anthracenedimethanol was prepared by a one pot stereoselective double reduction in good yield and excellent enantiomeric excess. We examined the association with *ortho*- and *meta*-benzenedimethanol showing bidentate complexes stable enough to be studied by low temperature NMR. Molecular modeling helped us to propose an association complex.

1. Introduction

NMR spectroscopy in chiral solvents allows enantiomers to be distinguished thus providing the means for the assignment of their stereochemistry.[1] The utilization of chiral solvating agents (CSA) is a very common and powerful technique to assess the composition of mixtures of enantiomers[2] by NMR spectroscopy. Chiral oriented phases[3] afford a new way to differentiate chiral molecules.

We have previously reported[4] the preparation of the enantiomers of α,α′-bis(trifluoromethyl)-9,10-anthracenedimethanol **1**, which present very high CSA activities that justify their commercialization. We extended this study to the preparation and evaluation of the CSA activity of α,α′-bis(trifluoromethyl)-10,10′-(9,9′-bianthryl)dimethanol **2**.[5] Further improvements in the methodology necessitated systematic spectral studies of substrate/CSA complexes, as well as deeper insights into the interactions responsible for their formation. We herein report these phenomena separately from the chirality of the substrates, isolating the association of the discrimination. The observed chemical shifts in the conditions of a substrate/CSA association depend on the inherent chemical shifts of the complex and on the equilibrium constant for the complex formation and dissociation. Since the nature of the forces responsible for the association of two enantiomers should be very similar, we expect that the differences between the equilibrium constants are also small.[4] The difference in the magnetic properties of individual complexes is the dominating factor that determines enantiodifferentiation. Differences in the geometries of the complexes and the magnetic anisotropy provide sufficient conditions for enantiodifferentiation to be registered by NMR.

An important factor in enhancing the enantiodiscrimination capacity of compound **1** is the symmetrical double functionality. The recognition of a stereogenic center is normally described[6] by a three-point interaction of different character. The presence of the two hydroxyl groups at the two stereogenic centers assures easy and an effective formation of a bidentate complex[7] that, through the intermediacy of a third interaction (e.g., between the aromatic rings)[8] makes chiral separation possible. Moreover, closer proximity between the components of the bidentate complex increases their magnetic influence and, accordingly, the differentiation. Considering compound **1** as a *para*-substituted aromatic hydrocarbon, we attempted the analyses (by NMR and molecular mechanics modeling) of the bidentate complexes of **1** with two standard compounds, the *ortho*- and *meta*-benzenedimethanol, **3** and **4**, respectively. These compounds afford complexations that differ significantly from the corresponding self-associations. Due to the insolubility of the *para*-benzenedimethanol **5**, the

* Corresponding author. Tel.: +34-93-5812924; fax: +34-93-5811265; e-mail: albert.virgili@uab.es

0957-4166/$ - see front matter © 2004 Elsevier Ltd. All rights reserved.
doi:10.1016/j.tetasy.2004.03.019

corresponding association with **1** was studied only by molecular mechanics modeling.

2. Results and discussion

2.1. Enantioselective synthesis of α,α′-bis(trifluoromethyl)-9,10-anthracenedimethanol 1 and α,α′-bis(trifluoromethyl)-10,10′-(9,9′-bianthryl)dimethanol 2

The described[4] preparation of the enantiomers (*R*,*R*)-**1** and (*S*,*S*)-**1** necessitates a final separation process by chiral HPLC, where 50% of the compound is lost in the *meso* form. We thus attempted an 'enantioselective' synthesis in order to optimize the preparation.

The enantioselective reduction of prochiral ketones[9] is one of the most useful methods for obtaining enantiomerically enriched alcohols. Several stoichiometric and catalytic methods have been developed. Enzymatic reduction,[10] the use of modified aluminum hydrides[11] and modified boron hydrides[12] afford very useful enantioselective synthetic methods.

A CBS reaction,[13] where a ketone is reduced by a borane with the addition of catalytic amounts of a chiral oxazaborilidine, is one of the most efficient catalytic processes. Many applications of the method,[14] including the case of 9-trifluoacetylanthracene,[15] were reported with very good yields and excellent enantiomeric excesses. However, only a few diketone compounds have been described.[16] In this case, while the first reduction is an enantioselective process, the second one can be considered as a diastereoselective reaction. If accounting for the statistical factors, only diastereoisomeric impurities should be detected in a double reduction of a diketone. We applied this reduction to 9,10-bis(trifluoroacetyl)anthracene **6** (Scheme 1) and to 10,10′-bis(trifluoroacetyl)-9,9′-bianthracenyl **7**.

The reaction of anthracenic diketone **6** yielded a mixture of the mono-reduction **8** and the di-reduction **1** compounds in a ratio that depended strongly on the experimental conditions (Table 1). After the analysis of the influence of several factors (temperature, concentration, reactants ratio), we optimized the conditions for a maximum yield of the di-reaction[17] when either the (*R*)- or (*S*)-methyl oxazaborolidine (tetrahydro-1-methyl-3,3-diphenyl-1H,3H-pyrrolo[1,2-*c*][1,3,2]oxazaborole) was used. High concentration of the starting compound **6** was a crucial factor for the formation of **1**. The control of the enantiomeric excess was carried out by analysis of the corresponding acetate derivative by HPLC in a Welch-O1 column with it always being more than 98%. The reaction proceeded with good yields using 10g of **2**. Reduction of **7** was carried out in the optimized conditions obtaining a mixture of mono and di-reacted **2** compounds. However only the latter could be isolated.

2.2. Association study

The conformational equilibrium of compound **1** can be represented by two forms, a *cisoid* form and a *transoid*

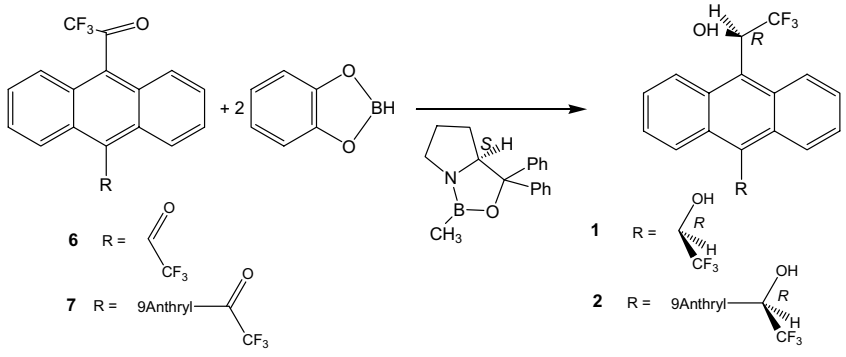

Scheme 1. Enantioselective preparation of **1** and **2**.

Table 1. Influence of the experimental conditions on the enantioselective reduction of diketone **6**

Entry	**6**/mmol	Tol/mL	Bor/mmol	Cat./mmol	T/K	Yield/%
1	0.4	30	1.6 (CB)	0.08	195	50% **8**
2	0.4	30	1.6 (CB)	0.08	253	30% **8**
3	0.4	30	1.6 (CB)	0.16	195	80% **8**
4	0.15	20	0.6 (CB)	0.15	195	70% **8**
5	0.27	40	1 (CB)	0.4	195	30% **8**
6	0.27	33	1 (CB)	0.4	195	90% **8**
7	2	80	8 (CB)	0.6	195	80% **1** 20% **8**
8	0.27	33	2 (DEANB)	0.2	295	60% **1** 40% **8**
9	0.15	33	2 (BH3.THF)	0.4	295	55% **1** 45% **8**

CB: catecholborane; DEANB: diethylanilineborane.

form[4] (Fig. 1). These two conformers are distinguishable by low temperature (250 K) ^{1}H NMR, where no variation is observed with the concentration.

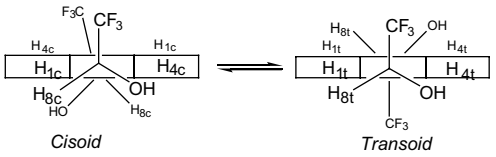

Figure 1. Vertical view of two conformations of enantiomer (*R*,*R*)-**1**.

The formation of bidentate complexes requires the simultaneous participation of two functional groups (hydroxyl), necessitating the involvement of the *cisoid* conformation. We observed a clear difference between the behavior of the two conformers of (*R*,*R*)-**1** in association with the *o*-benzenedimethanol **3**. While the *cisoid* form underwent a significant shift in magnetic shielding, the signals for the *transoid* conformation practically remained at the same positions.

A shift in the conformational equilibrium was also registered: the population ratio *cisoid*-**1**/*transoid*-**1** changed from 1.4 to 3.3 when increasing the concentration of **1**. These changes are produced by the formation of the complex with the participation of **1** in the *cisoid* conformation.

Figure 2 shows the ^{1}H NMR spectra at 250 K for the study of the formation of the complex between **1** and **3** for several concentration ratios.

Besides the hydroxyl protons, important shifts were registered for the H_{1c} and H_{8c} protons of **1**, and $H_{2'}$ and $H_{3'}$ of **3**.

All shifts are towards higher fields, that is, the nuclei are situated at positions where they are influenced by the anisotropic shielding zone of the other component of the complex.

The enantiotopic protons $H_{3'}$ were only weakly differentiated.

Again, we only observed the participation of the *cisoid* conformer of (*R*,*R*)-**1** in the complex with *m*-benzenedimethanol **4**. The ratio *cisoid*-**1**/*transoid*-**1** increased from 1.4 to 2.6 at the equimolar mixture of the two components. Figure 3 presents the ^{1}H NMR spectra at 250 K of the complex formation between **1** and **4** for several concentration ratios.

H_{1c} and H_{8c} are also the most significantly modified protons of *cisoid*-**1** in this case. The $H_{2'}$, $H_{3'}$ and largely $H_{1'}$ of **4** are strongly shifted. The *pro*-chiral benzylic protons have also changed the positions of their chemical shifts and enantio-recognized, obtaining an AB system after the addition of (*R*,*R*)-**1**.

The proximity between several protons of the two components has been manifested in the NOE spectra. The aromatic absorptions of **3** and **4** increased when H_1 and H_8 were saturated. Also, the methylene protons $H_{3'}$ of **3** showed NOE with H_8 of **1**. Figure 4 presents the intra and intermolecular nuclear Overhauser effect when the selective 1D NOESY[18] was measured. Although an equilibrium between the *cisoid* and the *transoid* conformations is present, so are saturation transfer and NOE transfer phenomena.

Due to the presence of several species, various equilibrium processes (conformational and association) and diverse points of the association, we had to interpret the results of the thermodynamic studies with some care. The evaluation of the stoichiometry of the process of formation of bidentate complexes was carried out on the basis of the Job[19] methodology; considering only the concentration of the *cisoid*-**1** component of the equilib-

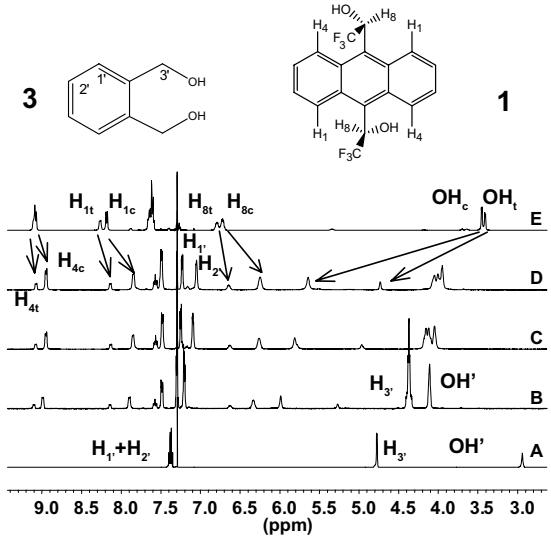

Figure 2. ^{1}H NMR spectra (250 K) of association between compounds *R*,*R*-**1** and **3**. A, pure **3**; B, [**1**]/[**3**] = 0.5; C, [**1**]/[**3**] = 1; D, [**1**]/[**3**] = 1.5; E, pure **1**.

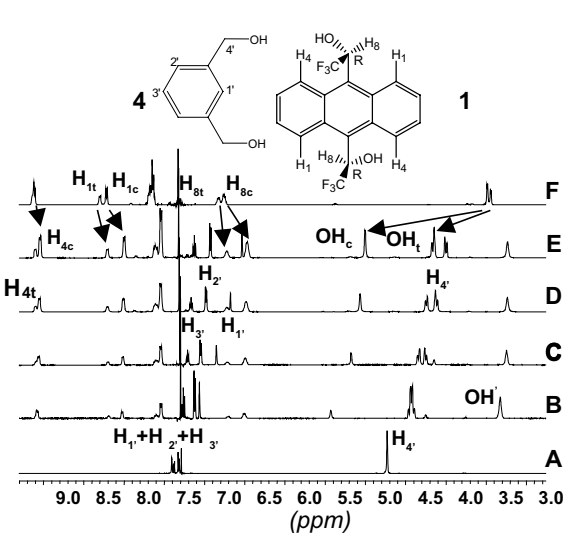

Figure 3. ^{1}H NMR spectra (250 K) of the association between compounds *R*,*R*-**1** and **4**. A, pure **4**; B, [**1**]/[**4**] = 0.5; C, [**1**]/[**4**] = 1; D, [**1**]/[**4**] = 1.5; E, [**1**]/[**4**] = 2; F, pure **1**.

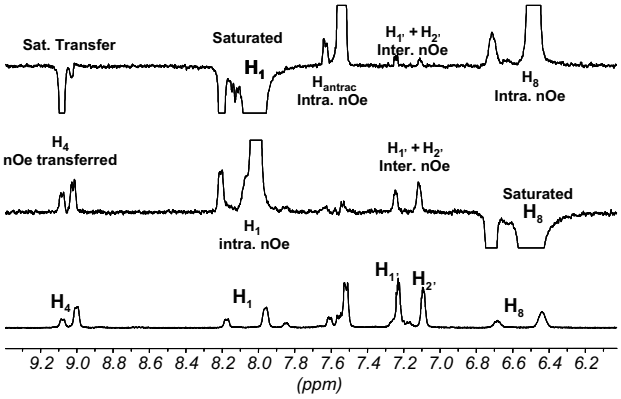

Figure 4. 1D NOE spectra of the association between (*R*,*R*)-**1** and **3**. The spectra were obtained using 1D DPFGNOE sequence at 250 K.

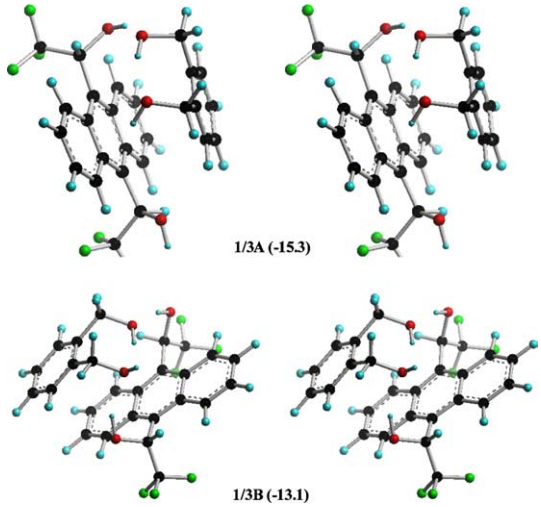

Figure 5. Stereoviews of the lowest energy structures for the associations of **3** with **1**. The computed energies of complex formation are given in parenthesis (in kcal mol^{-1}).

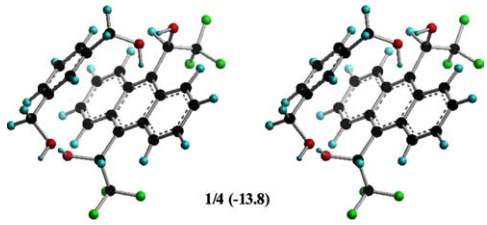

Figure 6. A stereoview of the lowest energy structure for the associations of **4** with **1**. The computed energies of complex formation are given in parenthesis (in kcal mol^{-1}).

rium. In the case of the association between (*R*,*R*)-**1** and **3**, and from the data for several protons, we obtained a maximum value of 0.5 from the Job plot (of the fitted quadratic function), corresponding to a 1:1 association. A slight deviation was present in the case of (*R*,*R*)-**1** and **4**, where the maximum value (of the fitted polynomial function) shifted to 0.6. Since we found the same value both for the protons of **1** and for the protons of substrate **4** (it has to be very different for ternary complexes), we can assume that other processes also have an influence and distort the Job correlation. Moreover, the small shift of the signals corresponding to *transoid*-**1** was greater in the case of the complexation of **4** than for the complexation of **3**, indicating an increased contribution of another mode of association different from the bidentate complexation.

The evaluation of the global binding constant by the equimolar method[20] yielded small values for the complexation between **1** and **3**, which increased with lowering of the temperature. The measure was made for protons H_{1cis}, H_{8cis} of **1** and methylene protons of **3**, obtaining average values of 8.7, 12.9, and 24.2 M^{-1} at 260, 250, and 240 K, respectively. Several attempts for analogous measurements of the association between **1** and **4** failed to produce values that could fit on a straight line in the equimolar method equation.

The MACROMODEL and BATCHMIN V5.0 software packages were used for the molecular modeling studies,[21] with the AMBER* all-atom force field[21,22] and the GB/SA (cavity + van der Waals + electrostatic polarization term) solvation model to simulate $CHCl_3$.[23–25] A dielectric constant of 1.0 was used for estimating the electrostatic interactions. Extended nonbonded cut-off distances were set to 10.0 Å for the van der Waals and 20.0 Å for the electrostatic interactions.

Two different modes of binding were detected for the association between **1** and **3** (Fig. 5, complexes **1/3A** and **1/3B**), while only one minimum energy structure was found in the case of the interaction with the *meta* derivative **4**, **1/4** (Fig. 6). Complex **1/3B** has relative energy 2.2 kcal mol^{-1} higher than complex **1/3A**. Moreover, **3** makes a more stable complex (**1/3A**) with **1** than **4** (**1/4**), $\Delta E = 1.5$ kcal mol^{-1}. The nonbonded (van der Waals and electrostatic) interactions favor complex **1/3A**, while the solvation energy terms enhance the formation of complex **1/4**.

The internal energy contributions (stretching, bending, and torsion) almost balance each other. Estimates of the energies of the complexes with higher values of the dielectric constant, $\varepsilon = 2.0$, retained the same order of stability of the structures. The two lowest energy complexes of **3** and **4** with **1** have completely different modes of binding and different patterns of hydrogen bonding that determine the geometries of the two complexes, **1/3A** and **1/4**. Two symmetrical hydrogen bonds are formed in **1/4** between the hydroxyl groups of **1** and the oxygen atoms of **4** with O–H···O contacts 1.83 Å.

The higher energy complex of **3** (**1/3B**) has a very similar pattern of complex formation: the same two hydrogen bonds as in **1/4** (1.88 and 1.93 Å), plus a hydrogen bond between the two hydroxyls of **3** (1.93 Å). Thus the oxygen atom of the *o*-hydroxyl group of **3** is equidistant (1.93 Å) from the two flanking hydroxyl groups (one from **1** and the other from **3**) while the three hydrogen bonds constitute a hydrogen bond relay system that may additionally stabilize the structure. Such a group-like behavior (cooperativity) of several hydrogen bonds is considered to strengthen the intramolecular hydrogen

bonding ('1 + 1 is more than 2'),[26] however, it is not modeled by the molecular mechanics force field. It is hard to believe that this energy stabilization could reverse the order of relative stability of the complexes of **3**.

The structural motif portrayed by the bidentate complex **1/3A** is completely different and the most interesting. Different balances of interactions determine its formation and stability. One of the hydroxyl groups of **3** interconnects by two hydrogen bonds (distances 1.86 Å) one of the hydroxyls of **1** and the other hydroxyl group of **3**. The hydrogen atom of the latter hydroxyl group is at distances ca. 2.6 Å from four aromatic carbon atoms of **1** (O–H···π hydrogen bonding). The other hydroxyl group of **1** establishes a favorable orientation towards its geminal trifluoromethyl group and the closest O–H···F contact is 2.3 Å. Thus, in addition to the van der Waals interactions, three specific favorable modes of interactions determine the structural motif presented by complex **1/3A** and its energy preference: O–H··· (OH, π, F) hydrogen bonds.

The geometries of the complexes **1/3A** and **1/4** are in accord with the monitored chemical shifts and the NOE spectra. $H_{2'}$ of **3** is the closest one positioned to H_{1c} and H_{8c} of **1**, and the three hydrogen atoms form a triangle with sides 3.3, 2.7, and 2.0 Å, respectively. The analogous triangle in the complex **1/4** is with sides 3.7, 3.0, and 2.0 Å. Inspection of the projections of **3** and **4** on **1** displays the arrangements of the protons with respect to the anisotropic shielding zones, which do not contradict the spectral observations.

The association of *para*-benzenedimethanol **5** with **1** was also studied with molecular mechanics. Two low-energy complexes of similar energies were found in this case (Fig. 7). The energies for complexation of **1/5** are intermediate between the estimated quantities for **1/3** and **1/4**. The geometries of the complexes **1/5A** and **1/5B** differ by the modes of intermolecular hydrogen bonding. Two symmetrical hydrogen bonds are formed in **1/5A** with the hydroxyl groups of **1** acting as proton donors, while in **1/5B** one of the hydroxyl groups of **1** is also hydrogen bonded to the adjacent trifluoromethyl group. Molecular mechanics studies of the self-associations **3/3**, **4/4**, and **5/5** yielded energies of complexations 9.1, 10.7, and 7.7 kcal mol^{-1}, respectively. Thus, self-associations cannot perturb the preferred formation of complexes between **3**, **4**, and **5** with **1**. The lowest energy **1/1** complex has D_2 symmetry and energy of complexation 19.1 kcal mol^{-1}. The van der Waals interactions are about 5 kcal mol^{-1} more favorable in comparison with the complex next in energy. Three **1/1** complexes were also found with higher relative energies 0.7–0.9 kcal mol^{-1}. The three lowest-energy **1/1** complexes have two O–H···O hydrogen bonds and two O–H bonds pointing towards its geminal trifluoromethyl groups. O–H···O, O–H···F, and O–H···π interactions determine the structure of the **1/1** complex with relative energy 0.9 kcal mol^{-1}.

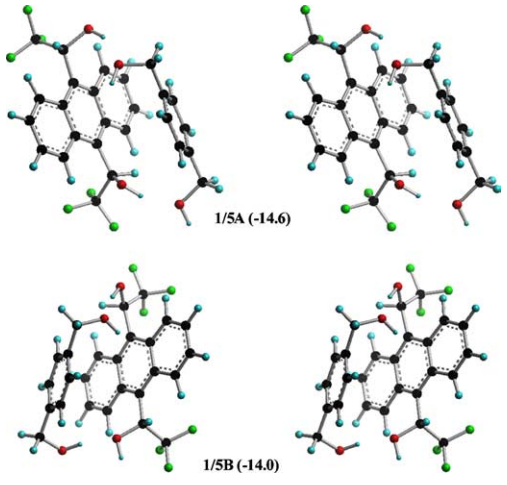

Figure 7. Stereoviews of the lowest energy structures for the associations of **5** with **1**. The computed energies of complex formation are given in parenthesis (in kcal mol^{-1}).

3. Experimental

3.1. General procedures

Nuclear magnetic resonance spectra were acquired at 11.75 T magnetic field strength instrument operating at ^{1}H frequency of 500 MHz and ^{13}C frequency of 125 MHz in solutions of $CDCl_3$ (referenced at 7.26 ppm for ^{1}H and 77.00 ppm for ^{13}C) or $(CD_3)_2SO$ (referenced at 2.49 ppm for ^{1}H and 39.50 ppm for ^{13}C).

3.2. Enantioselective reduction of diketones. General procedure

Under a nitrogen atmosphere, the catalyst (*S*)-methyl oxazaborolidine (0.6 mmol) was added to a stirred solution of diketone **6** (prepared as before[4]) (2 mmol) in anhydrous toluene (80 mL). After cooling to 80 °C the borane reducing agent (catecholborane, 0.5 mmol) was slowly dropped. The progress of the reaction was followed by gas chromatography until a constant ratio of mono- and di-reacted compounds. The mixture was washed with NaOH solution (10%) and after neutralization, the organic layer dried and evaporated. By silica gel column chromatography (hexane/CH_2Cl_2, 70:30), the resulting compounds (*R*,*R*)-α,α′-bis(trifluoromethyl)-9,10-anthracenedimethanol[4] **1** (80%) and (*R*)-2,2,2-trifluoro-1-[10-(2,2,2-trifluoro-1-hydroxyethyl)-9-anthrylethanone **8** (20%) were isolated and purified. The enantiomeric excess of both compounds was measured through a diacetate derivative by chiral HPLC using a Whelk-O1 column using hexane/2-propanol (3 mL/min of 90/10 for di-reacted **1** compound and 2.4 mL/min of 98/2 for mono-reacted **8** compound) obtaining at least 98% ee.

Under the same conditions, diketone **7** (prepared as before[5]) afforded the compound corresponding to the reduction of both carbonyl groups α,α′-bis(trifluoromethyl)-10,10′-(9,9′-bianthryl)dimethanol[5] **2**. Yield 56%, ee 97%. The mono-reduced compound was detected but not isolated.

3.3. *R*-2,2,2-trifluoromethyl-10-(2,2,2-trifluoro-1-hydroxyethyl)-9-anthracenylketone 8

Mp 186–188 °C. EM (EI) m/z (%): 372 (44) (M), 303 (100), 234 (18), 206 (64%), 178 (38). IR (KBr)/cm^{-1}: IR (KBr) cm^{-1}: 761, 1114, 1155, 1219, 1255, 1451, 1733, 2853, 2924, 3528. ^1H NMR (400 MHz, CD_3COCD_3, 270 K) δ (ppm): 9.32 (H_4, 1H), 8.65 (H_5, 1H), 7.75 (H_1, H_2, H_3, H_6, H_7, H_8, m, 6H), 7.24 (OH, d, $J_{OH/H11} = 5{,}9$, 1H), 7.00 (H_{11}, q, $J_{H11/F} = 5.9$, 1H).

Acknowledgements

Financial support from CICYT (project 2000-369) is gratefully acknowledged. CIRIT (Generalitat de Catalunya, Catalonia, Spain) and the MECD (Spain) are also acknowledged for Visiting Professor grants to one of us (P.I.).

References and notes

1. (a) Kobayashi, Y.; Hayashi, N.; Choon-Hong, T.; Kishi, Y. *Org. Lett.* **2001**, *3*, 2245–2248; (b) Hayashi, N.; Kobayashi, Y.; Kishi, Y. *Org. Lett.* **2001**, *3*, 2249–2252; (c) Hayashi, N.; Kobayashi, Y.; Kishi, Y. *Org. Lett.* **2001**, *3*, 2253–2255.
2. (a) Parker, D. *Chem. Rev.* **1991**, *91*, 1441–1457; (b) Wenzel, T. J.; Wilcox, J. D. *Chirality* **2003**, *15*, 256–270.
3. (a) Aroulanda, C.; Merlet, D.; Courtieu, J.; Lesot, P. *J. Am. Chem. Soc.* **2001**, *123*, 12059–12066; (b) Lesot, P.; Sarfati, M.; Courtieu *J. Chem. Eur. J.* **2003**, *9*, 1724–1745.
4. Pomares, M.; Sánchez-Ferrando, F.; Virgili, A.; Alvarez-Larena, A.; Piniella, J. F. *J. Org. Chem.* **2002**, *67*, 753–758.
5. Sánchez-Aris, M.; Estivill, C.; Virgili, A. *Tetrahedron: Asymmetry* **2003**, *14*, 3129–3135.
6. Pirkle, W. H.; Hoover, D. J. *Top. Stereochem.* **1982**, *13*, 263–331.
7. Mazik, M.; Radunz, W.; Sicking, W. *Org. Lett.* **2002**, *4*, 4579–4582.
8. Meyer, E. A.; Castellano, R. K.; Diederich, F. *Angew. Chem., Int. Ed.* **2003**, *42*, 1210–1250.
9. Itsuno, S. *Org. Reac.* **1998**, *52*, 395–576.
10. Csuk, R.; Glänzer, B. I. *Chem. Rev.* **1991**, *91*, 49–97.
11. Chong, J. M.; Mar, E. K. *J. Org. Chem.* **1991**, *56*, 893–896.
12. Ramachandran, P. V.; Teodorovic, A. V.; Brown, H. C. *Tetrahedron* **1993**, *49*, 1725–1738.
13. Corey, E. J.; Bakshi, R. K.; Shibata, S. *J. Am. Chem. Soc.* **1987**, *109*, 5551–5553.
14. Corey, E. J.; Helal, C. J. *Angew. Chem., Int. Ed.* **1998**, *37*, 1986–2012.
15. Corey, E. J.; Bakshi, R. K. *Tetrahedron Lett.* **1990**, *31*, 611–614.
16. Prasad, K. R. K.; Joshi, N. N. *J. Org. Chem.* **1996**, *61*, 3888–3889.
17. $T = 195$ K, [3] = 3.3 mg/mL, 4 equiv of cathecholborane, 0.6 equiv of oxazaborolidine.
18. Stott, K.; Stonehouse, J.; Keeler, J.; Hwang, T. L.; Shaka, A. J. *J. Am. Chem. Soc.* **1995**, *117*, 4199–4200.
19. Job, P. *Ann. Chem.* **1928**, *9*, 113–203.
20. (a) Bouquant, J.; Chuche, J. *Tetrahedron Lett.* **1972**, *23*, 2337–2340; (b) Raber, D. J.; Hardee, L. E. *Org. Magn. Reson.* **1982**, *20*, 125–132; (c) Fielding, L. *Tetrahedron* **2000**, *56*, 6151–6170.
21. Mohamadi, F.; Richards, N. G. J.; Guida, W. C.; Liskamp, R.; Caufield, C.; Chang, G.; Hendrickson, T.; Still, W. C. *J. Comput. Chem.* **1990**, *11*, 440–467.
22. Weiner, S. J.; Kollman, P. A.; Nguyen, D. T.; Case, D. A. *J. Comput. Chem.* **1986**, *7*, 230–252.
23. Hasel, W.; Hendrickson, T. F.; Still, W. C. *Tetrahedron Comput. Method.* **1988**, *1*, 103–116.
24. Still, W. C.; Tempczyk, A.; Hawley, R. C.; Hendrickson, T. *J. Am. Chem. Soc.* **1990**, *112*, 6127–6129.
25. Nagy, P. I.; Bitar, J.; Smith, D. A. *J. Comput. Chem.* **1994**, *15*, 1228–1240.
26. Prins, L. J.; Reinhoudt, D. N.; Timmerman, P. *Angew. Chem., Int. Ed.* **2001**, *40*, 2382–2426.